

# ***The Oaxaca Earthquake of 30 September 1999 ( $M_w = 7.5$ ): A Normal-faulting Event in the Subducted Cocos Plate***

**S. K. Singh<sup>1,2</sup>, M. Ordaz<sup>2</sup>, L. Alcántara<sup>2</sup>, N. Shapiro<sup>1</sup>, V. Kostoglodov<sup>1</sup>, J. F. Pacheco<sup>1</sup>, S. Alcocer<sup>2,3</sup>, C. Gutiérrez<sup>3</sup>, R. Quaas<sup>2,3</sup>, T. Mikumo<sup>1</sup>, and E. Ovando<sup>2</sup>**

UNAM and CENAPRED Seismology Group

**Contributions were made (in alphabetical order) by J. Aguirre<sup>2</sup>, D. Almora<sup>2</sup>, J. G. Anderson<sup>4</sup>, M. Ayala<sup>2</sup>, C. Javier<sup>5</sup>, G. Castro<sup>2</sup>, R. Duran<sup>3</sup>, G. Espitia<sup>3</sup>, J. Estrada<sup>1</sup>, E. Guevara<sup>3</sup>, J. Lermo<sup>2</sup>, B. Lopez<sup>3</sup>, O. Lopez<sup>3</sup>, M. Macías<sup>2</sup>, E. Mena<sup>5</sup>, M. Ortega<sup>3</sup>, C. Perez<sup>2</sup>, J. Perez<sup>1</sup>, M. Romo<sup>2</sup>, M. Ramírez<sup>3</sup>, C. Reyes<sup>3</sup>, R. Ruiz<sup>3</sup>, H. Sandoval<sup>2</sup>, M. Torres<sup>2</sup>, E. Vázquez<sup>2</sup>, R. Vázquez<sup>2</sup>, J. M. Velasco<sup>2</sup>, and J. Ylizaturri<sup>2</sup>**

UNAM and CENAPRED Seismology Group

## **INTRODUCTION**

The two large earthquakes to occur in México in 1999 were both normal-faulting, intraplate events in the subducted Cocos Plate. There is, however, a significant difference in their locations with respect to the coast, and, hence, with respect to the strongly coupled plate interface. The 15 June 1999 Tehuacán earthquake ( $H \sim 60$  km;  $M_w = 7.0$ ) was located about 200 km inland from the coast (Singh *et al.*, 1999) and in this sense was a typical intraplate event in the subducted slab. The Oaxaca earthquake of 30 September 1999 ( $H \sim 45$  km;  $M_w = 7.5$ ), on the other hand, occurred almost below the coast. As we point out later, the 1999 Oaxaca earthquake is not unique; two other, recent intraplate events had similar characteristics. In some aspects the 1999 earthquake is similar to the great intraplate Oaxaca earthquake of 15 January 1931 ( $M = 7.8$ ), which caused great destruction in the state of Oaxaca, especially in the city of Oaxaca.

For the 1999 Oaxaca earthquake the National Seismological Service (SSN) of México reported a magnitude of 7.4 and assigned an epicentral location near the coastal town of Puerto Escondido. Since the real-time network coverage of SSN is poor, the depth of the earthquake was poorly determined. A coastal epicenter suggested a thrust earthquake on

the plate interface. It was not until the Harvard CMT solution became available that it was realized that it was a normal-faulting intraplate earthquake.

The earthquake caused serious damage in the state of Oaxaca. The heavy rains which preceded and followed the earthquake compounded the loss and presented enormous difficulties in providing emergency help. In this report, we present the plate tectonic framework of the region, the seismological aspects of the earthquake, an isoacceleration map, the attenuation of peak ground motion with distance, a description of the damage, and an isoseismal map.

## **PLATE TECTONIC FRAMEWORK AND SEISMICITY OF THE OAXACA REGION**

The Cocos Plate subducts beneath Oaxaca with a relative convergence rate of 6.4 cm/yr, resulting in large thrust earthquakes on the plate interface. The seismicity of Oaxaca is characterized by (a) relative simplicity of the sources of large thrust earthquakes (Singh and Mortera, 1991), (b) earthquake statistics providing strong evidence of characteristic earthquakes ( $M_w \sim 7.5$ ) in the region (Singh *et al.*, 1983), and (c) a relatively constant recurrence period of large thrust earthquakes (Singh *et al.*, 1981). A discussion of the seismicity of Oaxaca is given by Nuñez-Cornu and Ponce (1989).

Figure 1 shows aftershock areas of thrust earthquakes which have occurred since 1960 and epicenters of known normal-faulting events ( $M \geq 6.5$ ) of this century. A section across the subduction zone of Oaxaca is shown in Figure 1b. The

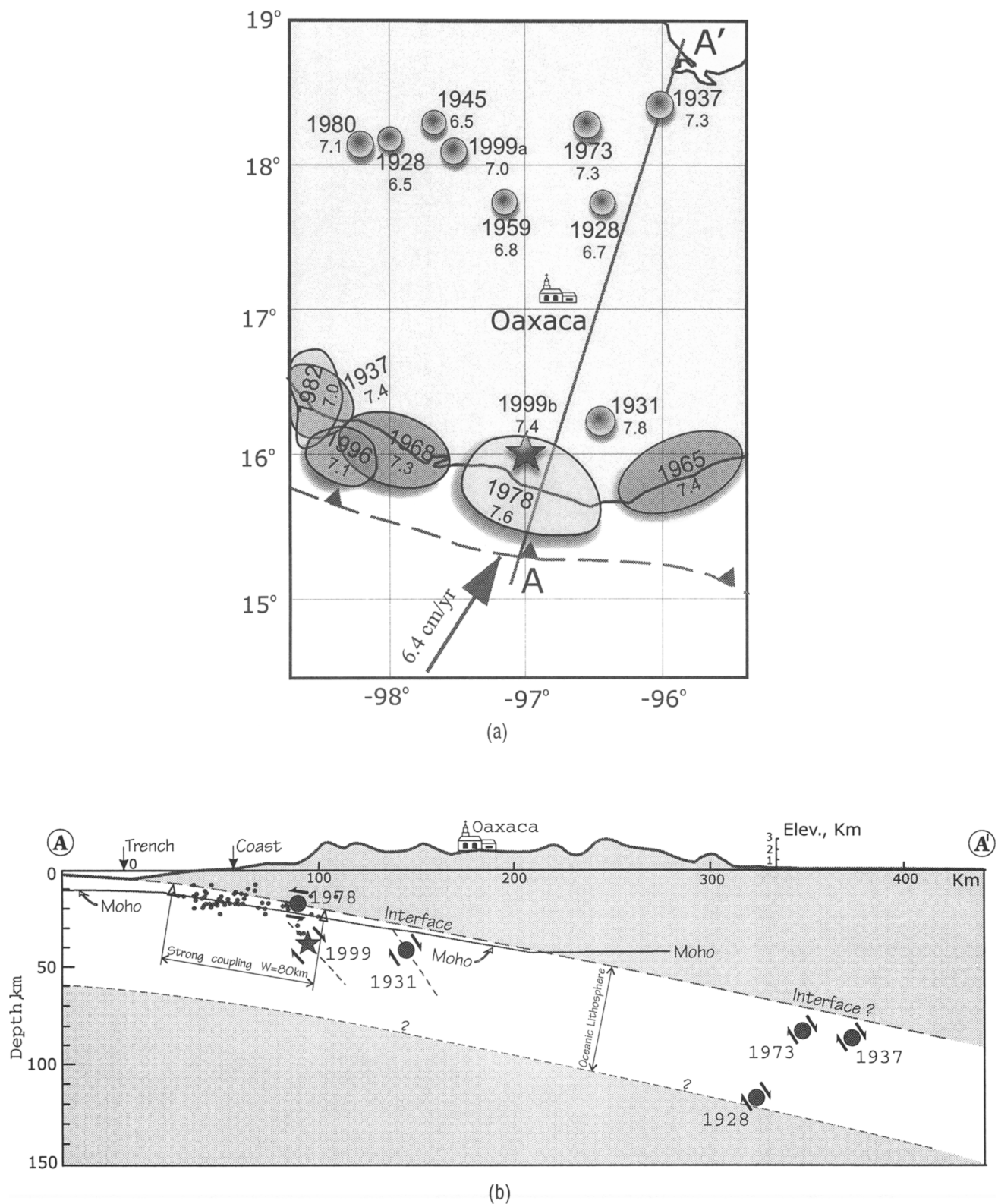
1. Instituto de Geofísica, UNAM, México

2. Instituto de Ingeniería, UNAM, México

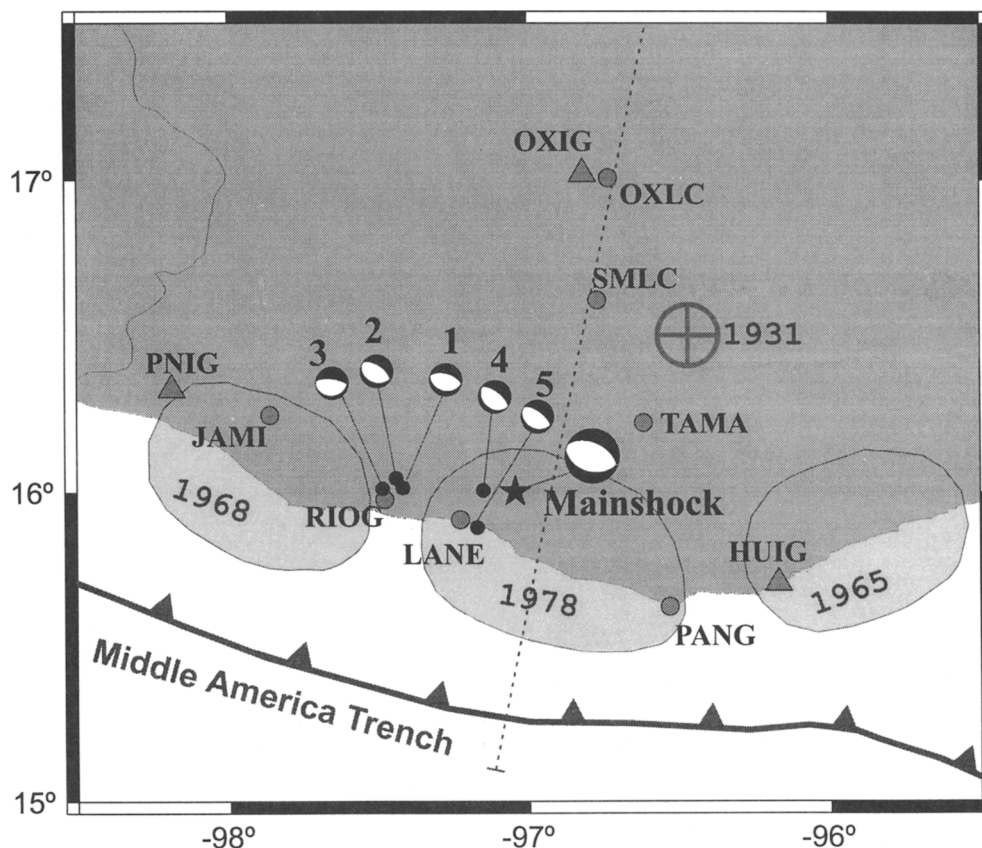
3. Centro Nacional de Prevención de Desastres, México

4. Seismological Laboratory, University of Nevada, Reno

5. Comisión Federal de Electricidad, México



▲ **Figure 1.** (a) Location map showing epicenter, magnitude, and year of significant normal-faulting earthquakes in the Oaxaca region (shaded circles). 30 September 1999 ( $M_w = 7.5$ ) is shown by a star. Aftershock areas of large thrust earthquakes which have occurred since 1960 on the Cocos-North American Plate interface are indicated by ellipses. The arrow gives the direction of relative plate convergence. Bottom: A section along AA' (modified from Singh *et al.*, 1985). Small circles denote aftershocks of the 1978 earthquake ( $M_w = 7.6$ ) and outline the zone of strong coupling. The star is the point of rupture initiation of the 30 September 1999 earthquake. The dip of the plate interface is  $\sim 15^\circ$ .



▲ **Figure 2.** A closer view of the region of interest. Stations near the epicenter are indicated by their four-letter codes. Shaded circles = accelerographs, shaded triangles = broadband stations equipped with velocity and acceleration sensors. The star is the epicenter of the mainshock determined from local/regional data. The mainshock focal mechanism is from the Harvard CMT solution. The locations and the focal mechanisms of five early aftershocks are based on the local data (Table 2). The broken line corresponds to AA' of Figure 1.

section includes aftershocks of the 1978 ( $M_w = 7.6$ ) thrust-faulting earthquake (Singh *et al.*, 1980). These aftershocks suggest that the downdip extent of the strongly coupled plate interface may be about 80 km. The subducted slab has a dip of  $\sim 15^\circ$ , defined by focal mechanisms of thrust earthquakes and location of normal-faulting earthquakes (see also Pardo and Suárez, 1995). The devastating 1931 Oaxaca earthquake was located between the coast and the city of Oaxaca.

## MAIN SHOCK

There were several digital accelerographs, equipped with GPS timing, and three broadband seismographs in the epicentral region which recorded the earthquake (Figure 2). The data acquisition system of the broadband seismograph is connected to velocity and acceleration sensors. The velocity sensors were clipped during the mainshock but the earthquake was well recorded on the acceleration channels. ( $S-P$ ) times were 5.2 s and 6.6 s at stations LANE and RIOG, respectively. In locating the mainshock and the aftershocks (see later section), we used a two-layer crust ( $\alpha_1 = 6.2$  km/s,  $H_1 = 15$  km;  $\alpha_2 = 6.85$  km/s,  $H_2 = 15$  km) overlying the mantle ( $\alpha_3 = 8.15$  km/s) and assumed a Poisson solid. This simplified

model is based on the results of a sea-land refraction profile about 120 km to the northwest of the epicenter (Valdés *et al.*, 1986). The mainshock epicenter and depth are relatively insensitive to minor variations of the crustal model because the depth of the event is strongly constrained by several  $P$  and  $S$  readings from several stations in the epicentral region.

Table 1 summarizes source parameters of the earthquake reported by different groups. The focal mechanisms, determined from the analysis of teleseismic data, are similar: a normal-faulting earthquake with strike parallel to the trench. The estimates of seismic moment vary between 1.1 to  $2.0 \times 10^{27}$  dyne-cm. The reported focal depths lie between 40 and 55 km. The shallowest depth is obtained from the local data and refers to the point of rupture initiation. The depth estimated from the teleseismic data corresponds to the centroid depth. If the depths are correct, then the rupture started at a depth of about 40 km but much of the slip occurred between 50 and 55 km.

## Source Characteristics

Local and regional data suggest that the rupture propagated toward the northwest, along the strike of the fault. For example, Figure 3 shows bandpass-filtered (0.05–0.2 Hz) dis-

TABLE 1. Source Parameters of the 30 September 1999 Oaxaca Earthquake							
Source	Lat	Long.	Depth (km)	Mo, dyne-cm	Strike	Dip	Rake
CMT <sup>a</sup>	16.23°N	96.97°W	53.9	$2.0 \times 10^{27}$	295°	50°	−82°
NEIC <sup>b</sup>	16.148°N	96.708°W	53.0	$1.4 \times 10^{27}$	315°	55°	−81°
Univ. of Michigan <sup>c</sup>	16.10°N	96.70°W	42.0	$1.1 \times 10^{27}$	294°	59°	−101°
Kikuchi <sup>d</sup>	16.10°N	96.70°W	55.0	$1.3 \times 10^{27}$	295°	51°	−83°
Local <sup>e</sup>	16.00°N	97.02°W	39.7	—	—	—	—

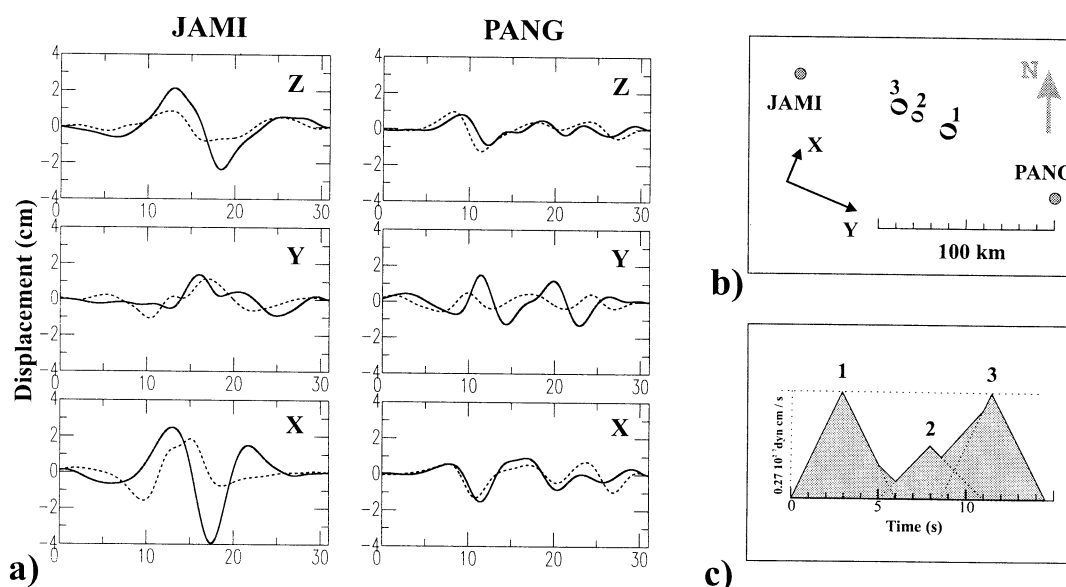
a. Preliminary Harvard CMT solution

b. Preliminary NEIC CMT solution

c. Source time function reported by the University of Michigan, source duration 17 s

d. From inversion of teleseismic body waves (M. Kikuchi, personal communication, 1999)

e. Epicentral location and depth from local/regional data



▲ **Figure 3.** (a) Bandpass (0.05–0.2 Hz) displacement seismograms at stations JAMI and PANG (continuous lines) and synthetic seismograms (dashed lines) corresponding to sum of three subevents whose locations are given in (b) and whose source time functions are shown in (c). The rupture initiated with subevent 1 and propagated northwest toward JAMI (b).

placement seismograms at stations JAMI and PANG, which are located along the strike of the fault (Figure 2). The seismograms at PANG indicate three subevents, while those at JAMI can be explained by a single event. Also the amplitudes are greater and the duration of the S wave is shorter at JAMI than at PANG. Source directivity toward the northwest would explain these observations.

We performed a forward modeling of the filtered displacement seismograms at PANG and JAMI. We fixed the depth of the subevents at 40 km and the focal mechanism to that given by the Harvard CMT solution (Table 1). The subevents were assumed to occur along the strike of the fault (295°), with the first subevent located at the hypocentral location (16.00°N, 97.02°W). The pulse duration of each subevent

was taken as 6 s. Synthetic seismograms were computed using Bouchon's (1982) algorithm. Figure 3a shows synthetics corresponding to three subevents, where the second and the third subevents events are located 21.9 and 31.4 km from the first (Figure 3b), acting 5.0 and 8.5 s after the first (Figure 3c). Thus the total rupture duration is 14.5 s. The seismic moments of the three subevents are 0.8, 0.4, and  $0.8 \times 10^{27}$  dyne-cm, giving total  $M_0 = 2.0 \times 10^{27}$  dyne-cm. As seen in Figure 3a, the synthetic seismograms fit the observed ones reasonably well, suggesting that the gross source characteristics are fairly well explained by the rupture scenario summarized in the figure. The result from body-wave inversion of teleseismic data is similar to that shown in Figures 3b and 3c (M. Kikuchi, personal communication, 1999).

## Source Spectrum and Seismic Energy Release from Local/Regional Data

The source spectrum of the Oaxaca earthquake was estimated from the horizontal recordings at TAMA, PANG, SMLC, HUIG, OXLC, and CHFL (Figure 2). We purposely neglected data from LANE and RIOG since the far-field approximation is grossly violated at these near-source stations. We also neglected JAMI because of possible large amplification of high-frequency seismic waves. The far-field Fourier acceleration spectral amplitude of the intense part of the ground motion,  $A_i(f, R_i)$ , at station  $i$ , which is located at a distance  $R_i$  from the source, can be written as

$$A_i(f, R_i) = \frac{C f^2 \dot{M}_0(f) e^{-\frac{\pi f R_i}{\beta Q}}}{G(R_i)}, \quad (1)$$

where

$$C = \frac{R_{\theta\phi} F P (2\pi)^2}{4\pi\rho\beta^3} \quad (2)$$

and  $\dot{M}_0(f)$  is the moment-rate (or source displacement) spectrum. In the limit,  $\dot{M}_0(f) \rightarrow M_0$  as  $f \rightarrow 0$ .

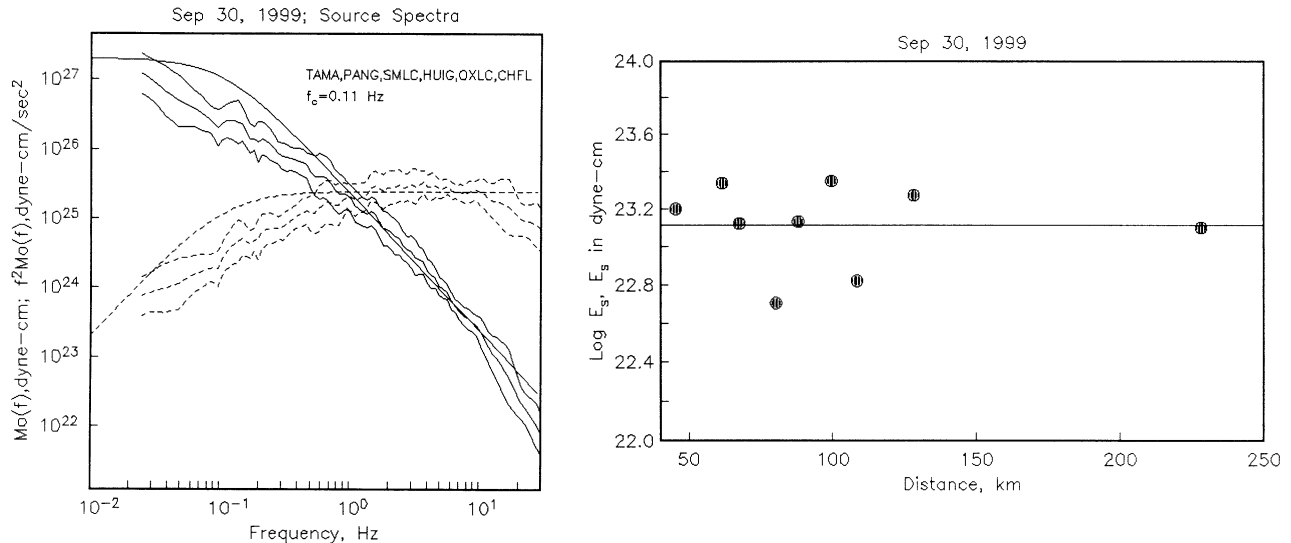
In the equations above,  $R_i$  is the hypocentral distance of the  $i$ th station,  $\beta$  is the shear-wave velocity,  $\rho$  is the density,  $Q(f)$  is the quality factor,  $R_{\theta\phi}$  is the average radiation pattern (0.55),  $F$  is the free surface amplification (2.0),  $P$  takes into

account the partitioning of energy in the two horizontal components ( $1/\sqrt{2}$ ), and  $M_0$  is the seismic moment of the earthquake.  $G(R)$  in equation (1) is the geometrical spreading term, which may be taken as  $G(R) = R$  for  $R \leq R_x$  and  $G(R) = (RR_x)^{1/2}$  for  $R > R_x$ . The form of  $G(R)$  implies dominance of body waves for  $R \leq R_x$  and of surface waves for  $R > R_x$ . For the Oaxaca earthquake, we took  $\beta = 4.70$  km/s,  $\rho = 3.2$  gm/cm<sup>3</sup>, and  $Q(f) = 273f^{0.66}$  (Ordaz and Singh, 1992) and set  $R_x = 300$  km, so that  $G(R) = R$  for all stations used in computing the source spectra.

The average source displacement and acceleration spectra,  $\dot{M}_0(f)$  and  $f^2 \dot{M}_0(f)$ , are shown in Figure 4a. The Figure also includes the  $\omega^2$ -source spectrum corresponding to  $M_0 = 2.0 \times 10^{27}$  dyne-cm and a tentatively estimated corner frequency,  $f_c$ , of 0.11 Hz. The spectrum with this corner frequency appears to fit the high-frequency radiation ( $1 \leq f \leq 10$  Hz) from the source (Figure 4a). We note, however, that the theoretical  $\omega^2$  spectrum corresponding to  $f_c = 0.11$  Hz overestimates the spectrum in the frequency range of 0.02 and 1 Hz. The corner frequency in the far-field spectrum may be related to the average stress drop,  $\Delta\sigma$ , as  $f_c = 4.91 \times 10^6 \beta (\Delta\sigma/M_0)^{1/3}$ , if we refer to Brune's model (1970), where  $\beta$  is the shear-wave speed in km/s.

At  $f \rightarrow 0.02$  Hz,  $\dot{M}_0(f)$  approaches a seismic moment of about  $1.0 \times 10^{27}$  dyne-cm. This value of  $M_0$  is consistent with those estimated from teleseismic body waves (Table 1).

$\Delta\sigma$  in these cases would be 216 bars for  $M_0 = 2.0 \times 10^{27}$  dyne-cm and 108 bars for  $M_0 = 1.0 \times 10^{27}$  dyne-cm if we use the above estimate of  $f_c$  with  $\beta = 4.7$  km/s.



▲ **Figure 4.** Left: Source displacement (continuous lines) and acceleration spectra (dashed lines),  $\dot{M}_0(f)$  and  $f^2 \dot{M}_0(f)$ , of the Oaxaca earthquake. Fit to the high-frequency spectra, assuming an  $\omega^2$ -source model and fixing  $M_0 = 2.0 \times 10^{27}$  dyne-cm, is shown by smooth curves and requires stress drop of ~230 bar. Median and  $\pm$  one standard deviation curves for each spectra are shown. Right: seismic energy,  $E_s$ , as a function of the hypocentral distance. The median value of  $E_s$  is  $1.3 \times 10^{23}$  erg.

## Source Energy Release from Local/Regional Data

We estimated the seismic energy,  $E_s$ , radiated during the Oaxaca earthquake from the relation (Singh and Ordaz, 1994):

$$E_s = \left\{ 4\pi R^2 \left[ \frac{G^2(R)}{R^2} \right] \frac{\rho\beta}{F_s^2} \right\} \left\{ 2 \int_0^\infty [V_N^2(f) + V_E^2(f) + V_Z^2(f)] e^{\frac{2\pi f R}{\beta Q(f)}} df \right\} \quad (3)$$

where  $V_j(f)$  is the velocity spectrum of the  $j$ th component. Figure 4b shows the plot of  $E_s$  as a function of distance  $R$ . The median value of  $E_s$  is  $1.3 \times 10^{23}$  ergs. The apparent stress,  $\sigma_a$ , is given by  $\sigma_a = \mu E_s / M_0$ . With  $\mu = 7.0 \times 10^{11}$  dyne/cm<sup>2</sup> and  $M_0 = 2.0 \times 10^{27}$  dyne-cm, the estimated value of  $\sigma_a$  is 46 bar. This value of the apparent stress is twice the value reported for shallow thrust earthquakes along the Mexican subduction zone (Singh and Ordaz, 1994). If the final stress equals the frictional stress (the Orowan model), then  $\Delta\sigma = 2\sigma_a = 92$  bar, where  $\Delta\sigma$  is the static stress drop. It is known that  $\Delta\sigma_B = 4.35\sigma_a$  (e.g., Singh and Ordaz, 1994), where  $\Delta\sigma_B$  is Brune's stress drop (Brune, 1970). This relation gives  $\Delta\sigma_B = 200$  bar, almost equal to the value of the stress drop needed to fit the high-frequency level of the source spectra.

On the other hand, Yagi and Kikuchi (1999) have derived the fault slip distribution from teleseismic waveform inversion. Our preliminary estimate of the maximum stress drop near the center of the fault is about 150 bars, if we refer to their results. We will also be making another waveform inversion of near-source strong-motion records to confirm the above results.

## AFTERSHOCKS

A portable network of digital seismographs and accelerographs was installed in the field to record aftershocks. The data collected by this network are presently being analyzed. SSN reports twenty-one aftershocks in twenty days with  $4.0 \leq M \leq 4.7$ . This aftershock activity is much greater than that observed following the 15 June 1999, Tehuacán earthquake ( $M_w = 7.0$ ,  $H = 60$  km), which was also a normal-faulting event in the subducted Cocos Plate. Perhaps the higher aftershock activity following the Oaxaca earthquake reflects its somewhat shallower depth.

Five of the larger aftershocks, which occurred within twenty-four hours of the earthquake, were recorded by the permanent accelerographs in the epicentral region and by the three broadband seismographs. All five events gave rise to accelerograms at LANE and RIOG (Figure 2). The aftershocks were located using the crustal model described above. The seismic moments and the focal mechanisms of these events were estimated by inverting displacement waveforms

recorded at near-source stations using a grid search method (Singh *et al.*, 1999). Figure 5a compares observed and synthetic waveforms of the largest aftershock ( $M_w = 4.65$ ). The fit is reasonable. The focal mechanism obtained from the inversion (Figure 5b) does not violate the available first-motion data.

The source parameters of the five aftershocks are listed in Table 2. The epicenters and the focal mechanisms are plotted in Figure 2. The focal mechanisms of the aftershocks are similar to the mainshock mechanism. We note the depths of four of the five aftershocks lie between 38 and 40 km. The minimum ( $S-P$ ) time of the five aftershocks is between 4.00 and 4.95 s, recorded either at LANE or at RIOG. This also suggests that the depth of these events was less than about 42 km. It seems that the aftershocks were mostly concentrated toward the upper edge of the rupture area, but this requires confirmation from a detailed analysis of the entire dataset. The mainshock and the aftershocks cover a length of ~50 km (Figure 2). The location of the main shock with respect to the aftershocks (Figure 2) suggests that the rupture propagated toward the northwest, along the strike of the fault. This is in accordance with the results of the forward modeling of the local data (Figure 3) and inversion of teleseismic body waves (M. Kikuchi, personal communication, 1999).

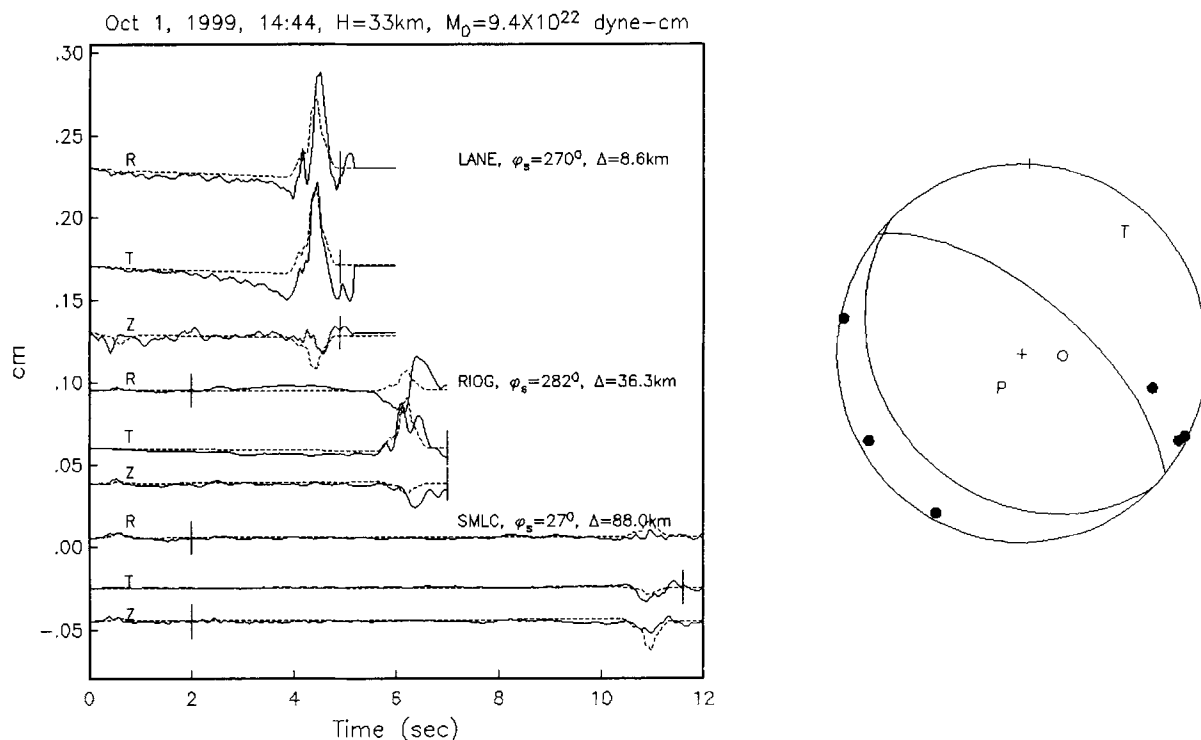
## SPATIAL AND TEMPORAL DISTRIBUTION OF INTERPLATE AND INTRAPLATE EARTHQUAKES IN OAXACA

Figures 1 and 2 show that the 1999 Oaxaca earthquake ruptured that part of the subducted slab which lies below the downdip edge of the strongly coupled interface.

It is interesting to examine the spatial and temporal characteristics of the 1999 Oaxaca earthquake. Intraplate earthquakes in the subducted slab, generally, occur downdip from the coupled interface, not immediately below or near the edge of it. The Oaxaca earthquake of 1999, however, is not the only exception. Of two recent, intraplate, normal-faulting earthquakes in the Michoacán-Guerrero region, one (11 January 1997,  $M_w = 7.1$ ) occurred just below the rupture area of the great 1985 ( $M_w = 8.0$ ) Michoacán earthquake, and the other (10 December 1994;  $M_w = 6.6$ ) just downdip from it.

Generally, the intraplate seismicity in subduction zones shows the following temporal behavior. (1) Prior to large/great thrust earthquakes on the plate interface, the events are tensional in the downdip subducted slab and compressional in the outer rise. (2) Following the rupture of the interface, the downdip events become either compressional or the tensional ones become less frequent, and the events in the outer rise become tensional. This pattern has been explained by locking and unlocking of the coupled plate interface (e.g., Astiz and Kanamori, 1986; Christensen and Ruff, 1988; Astiz *et al.*, 1988; Lay *et al.*, 1989).

For the Mexican subduction zone, Lay *et al.* (1989) reported that large, shallow thrust events were preceded by



▲ **Figure 5.** Left: Observed near-source displacement seismograms from three stations (continuous curves) of the aftershock of 1 October 1999, 14:14. Synthetic seismograms (dashed curves) correspond to the focal mechanism and the seismic moment obtained from inversion. The vertical line on each trace indicates the length of the record used in the inversion. Right: The focal mechanism obtained from the inversion. This mechanism does not violate the few available first-motion data and is similar to the mechanism of the mainshock.

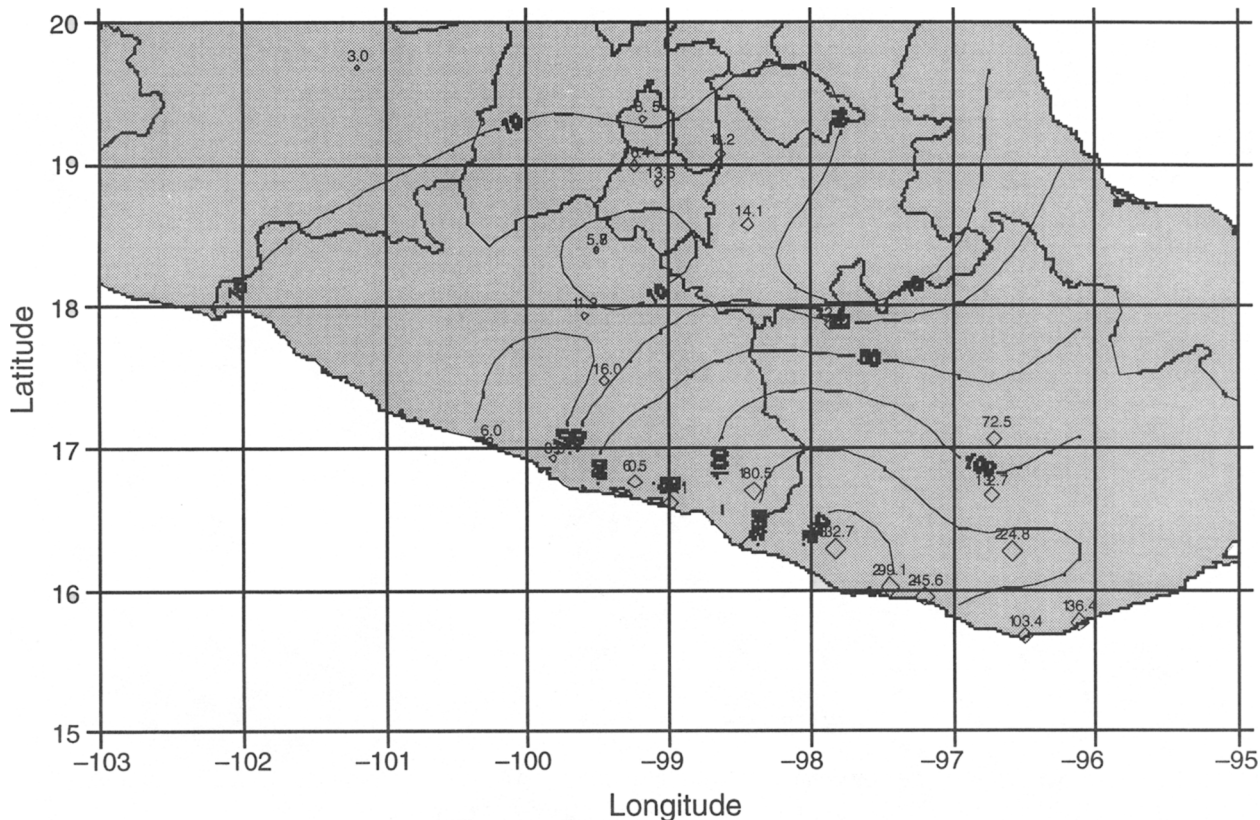
**TABLE 2.**  
**Early Aftershocks of the Earthquake**

No.	Date	Time	Lat.	Lon.	Depth (km)	Strike	Dip	Rake	$M_0$ (dyne-cm)	$M_w$
1	990930	16:50:57.2	16.069°N	97.356°W	36.2	286°	58°	-88°	$1.4 \times 10^{22}$	4.10
2	990930	19:04:44.7	16.099°N	97.373°W	37.1	305°	60°	-80°	$4.9 \times 10^{22}$	4.46
3	991001	00:30:42.3	16.066°N	97.419°W	36.8	277°	70°	-84°	$1.0 \times 10^{22}$	4.00
4	991001	03:33:38.0	16.061°N	97.084°W	38.2	307°	65°	-80°	$4.3 \times 10^{22}$	4.42
5	991001	14:44:10.6	15.939°N	97.105°W	32.4	307°	65°	-90°	$9.4 \times 10^{22}$	4.65

tensional downdip events, in accordance with the general pattern, but a decrease in the tensional events following the rupture of the interface was not clear from the available data. In fact, there is evidence that in México some large, downdip, tensional earthquakes follow shallow thrust earthquakes rather than precede them. For example, Singh *et al.* (1985) reported that the 1931 normal-faulting earthquake of Oaxaca occurred after four large thrust events ( $7.4 \leq M \leq 7.8$ ) ruptured the plate interface in the region in 1928. Similarly, the intraplate events of 1994 and 1997, mentioned above, also do not follow the general seismicity pattern since they occurred after the 1985 earthquake. Calculations by Mikumo *et al.* (1999) suggest that the 1997 near-vertical, normal-faulting earthquake could have been triggered by the increase in the static vertical shear stress in the subducted

slab caused by the 1985 earthquake. Cocco *et al.* (1997) speculated that the 1994 earthquake may have been caused by additional buckling of the subducted Cocos Plate in response to the sequence of several large updip, thrust earthquakes during 1979 and 1985.

The Oaxaca earthquake of 1999 occurred twenty-one years after the earthquake of 1978 ( $M_w = 7.6$ ). Since the recurrence period of large, thrust earthquakes in this segment of the subduction zone is about 54 years (Singh *et al.*, 1981), the 1999 event occurred roughly around midpoint of the earthquake cycle. Could this event be causally related to the 1978 earthquake? Preliminary calculations made by one of us (T. Mikumo) suggest that the 1978 earthquake may have caused an increase in the static shear stress of a few bars near the fault plane of the present event. It will also be inter-



▲ **Figure 6.** Isoacceleration map of the earthquake. The data from several stations to the west of 100°W were not available at the time of writing this report. Amax exceeded 300 gal in the epicentral region.

esting to compute the stress change caused by the 1999 earthquake. Will this event advance or delay the next thrust earthquake on the plate interface, which ruptured during 1978?

## ISOACCELERATION MAP

Figure 6 shows an isoacceleration map of the Oaxaca earthquake. The data from several stations, located west of 100°W, were not yet available at the time of writing this report. We note that Amax exceeded 300 gals in the epicentral region. As we show later, the 200-gal contour roughly coincides with the modified Mercalli intensity (MMI) of VII. It is clear from Figure 6 that a well distributed, dense network of strong-motion stations is still lacking in southern México to construct a reliable isoacceleration map.

### Amax versus Distance

Figure 7 shows that Amax data for the Oaxaca earthquake is a function of hypocentral distance,  $R$ . In this plot

$$A_{\max} = \sqrt{\frac{A_N^2 + A_E^2}{2}},$$

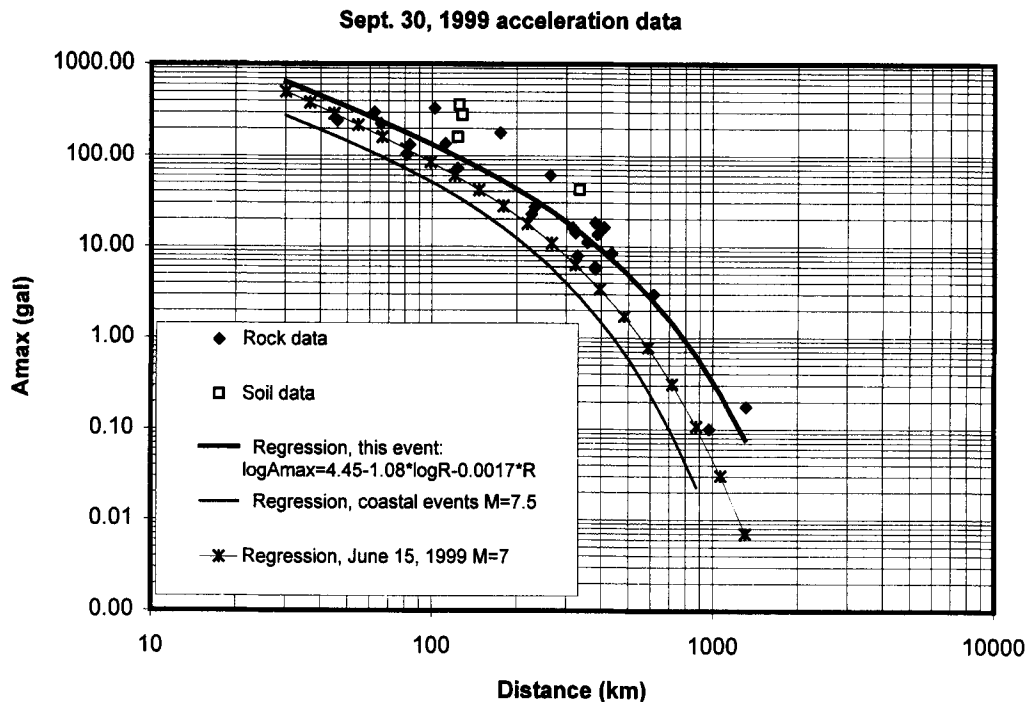
and  $A_N$  and  $A_E$  are peak ground accelerations in north-south and east-west directions, respectively. A regression analysis of the data from rock sites yields:

$$\log A_{\max} = 4.45 - 1.08 \log R - 0.0017R.$$

The figure includes the regression line corresponding to the 15 June 1999 Tehuacán earthquake ( $M_w = 7.0$ ), which was also an intraplate, normal-faulting event. As expected, Amax values are higher for the Oaxaca earthquake ( $M_w = 7.5$ ) as compared to the Tehuacán earthquake ( $M_w = 7.0$ ).

It is interesting to compare the regression line of the Oaxaca earthquake with that for a  $M_w = 7.5$  thrust earthquake on the plate interface of the Mexican subduction zone (Ordaz *et al.*, 1989). We note that the Amax values for the intraplate Oaxaca earthquake are at least twice the expected values of Amax for the interplate earthquake of the same magnitude (Figure 7). Even the Amax values for the  $M_w = 7.0$  Tehuacán earthquake are higher than those for a  $M_w = 7.5$  thrust event. This suggests that intraplate earthquakes in the subducted slab below México (and perhaps elsewhere in the world) are more energetic at higher frequencies than their shallower, thrust counterparts on the plate interface. This is also in agreement with higher stress-drop estimates for the Oaxaca earthquake as compared to a typical interplate Mexican earthquake, as mentioned earlier.





▲ **Figure 7.** Peak horizontal acceleration,  $A_{max}$ , versus focal distance,  $R$ , for the Oaxaca earthquake. Also shown in the figure are regressions for the 15 June 1999 Tehuacán ( $M_w = 7.0$ ) earthquake and for a shallow, interplate, thrust earthquake with  $M_w = 7.5$ .

Additional evidence of larger ground motions from intraplate earthquakes in the subducted slab as compared to those from interplate earthquakes comes from the relation between the magnitude,  $M$ , and area under modified Mercalli intensity contours,  $A_i$ . Singh *et al.* (1980) considered intensities IV, V, and VI and related  $M$  to  $A_i$  by  $M = \log A_i + C_i$ , where  $i$  is the MM intensity. They found that the constant  $C_i$  is about 0.6 less for intraplate as compared to interplate earthquakes. This implies that for the same magnitude, the area under intensities IV, V, and VI are about four times greater for intraplate as compared to interplate earthquakes.

## DAMAGE TO STRUCTURES AND LIFELINES

The high seismicity of the Oaxaca region has caused considerable damage to dwellings and churches in the past. It is evident that frequent and intense ground motions have modified construction practices in the region. Unlike in the adjacent state of Puebla (where the 15 June 1999,  $M_w = 7$  earthquake caused severe damage), the churches are shorter, sturdier, and stronger in Oaxaca. This partly explains why damage was not very severe to these structures. The damage was concentrated in nonengineered constructions, roads and bridges, and, to a lesser extent, historical monuments and engineered buildings. The damaged region extends considerably inland.

Damage was concentrated in the state of Oaxaca. In the city of Oaxaca, over 270 buildings have been reported damaged. One hospital suffered column damage and was evacuated. Some historical buildings, churches, and archaeological

sites such as Mitla and Monte Alban suffered damage. Over 150 churches throughout the state exhibited some problems. Cracking in arches and vaults due to flexural stresses was evident in most cases.

The most significant damage was observed in adobe houses that are typically made of walls without any horizontal or vertical reinforcement for continuity and confinement. Roofs are commonly made of wooden logs and boards that support inclined, and rather heavy, clay tile finishing. In some cases, walls failed; in others, the tiles slid. Typical wall damage was out-of-plane cracking and failure, as well as inclined cracking. Plain masonry wall structures also performed poorly due to lack of continuity and confinement. Government statistics indicate that over 41,000 houses were affected; just in San Pedro Tututepec, 3,200 houses were reported damaged and 3,000 were reported as collapsed.

Oaxaca's complex orography leads to a sparse distribution of towns and villages. Communication even in normal times is difficult. Heavy rains just a few days before the earthquake had damaged roads and bridges. Earthquake motions exacerbated the distress. Some towns were left inaccessible by land; 1,700 km of highways and rural routes were damaged. Landslides, longitudinal cracking of pavement, and undermining were typical. Subsequent continuous rains made the rehabilitation of the area very difficult.

Structural damage was recorded in engineered buildings. According to the federal government, over 1,500 schools were reported damaged; most of them have only cosmetic cracking. Hospitals and rural clinics were also reported damaged. Cracking in nonstructural elements was character-

istic; inadequate separation from the seismic-resistant structural system was apparent.

Phones and electricity services were disrupted after the earthquake in towns near the epicenter, as well as within the hilly areas.

In Mexico City, as anticipated, people exhibited anxiety and fear. Only one building was reported damaged. However, that structure was damaged in 1985 and rehabilitated with dubious success; it has been evacuated. More than half of the city experienced short-term blackouts. The subway system interrupted service for 8 minutes as part of its safety procedure; no damage was reported to the stations or the tracks. One hospital reported broken glass.

For comparison purposes, maximum acceleration recorded on the roof of a ten-story reinforced concrete structure in Mexico City, rehabilitated with external steel braces after 1985, was  $82 \text{ cm/s}^2$ , while during the 15 June 1999 Tehuacán earthquake it was  $122 \text{ cm/s}^2$ .

Minor damage was reported in five other states (Veracruz, Guerrero, Puebla, Tlaxcala, and Morelos). Very few of the churches damaged during the 15 June earthquake showed further deterioration.

According to official information the earthquake resulted in 35 deaths and 215 injuries.

## ISOSEISMAL MAP

An isoseismal map of the 1999 Oaxaca earthquake is shown in Figure 8. It was constructed using reports from local government authorities, telephone inquiries with civil protection agencies, newspaper accounts, e-mail messages, and reports from field inspection teams. The highest level of intensity on the modified Mercalli scale was VIII. This intensity was distributed in an area which coincides with the mainshock and aftershock epicenters (Figure 2) and, roughly, with the 200 gal isoacceleration contour (Figure 9). The earthquake was felt in high-rise buildings more than 800 km away from the epicenter.

Figure 8 also gives an isoseismal map of the 15 January 1931 ( $M_w = 7.8$ ) Oaxaca earthquake (Gutierrez and Miller, 1992), whose depth and focal mechanism were similar to that of 1999 (Singh *et al.*, 1985). During 1931 a maximum intensity of IX was reached in the epicentral area. The earthquake caused great destruction in the city of Oaxaca (Barrera, 1931). The higher magnitude of the 1931 event and its relatively closer location explains greater damage to the city in 1931 as compared to 1999. Due to low population density in 1931 in the surrounding states, the intensity contours are well defined mainly for the state of Oaxaca.

## CONCLUDING REMARKS

In the past five years, three significant, normal-faulting earthquakes in the subducted Cocos Plate, including the 1999 Oaxaca earthquake, have occurred below or near the

down-dip edge of the strongly coupled plate interface. Quite possibly such events are common in the subducted Cocos Plate but, in the past, have not been reported as such because of location errors. A satisfactory explanation of the extensional stress regime in the subducted slab below the coupled interface and the stress interaction and temporal relation between thrust events on the interface and normal-faulting events occurring below is still lacking and is beyond the scope of this report.

The data from the Tehuacán and the Oaxaca earthquakes of 1999 show that  $A_{max}$  from normal-faulting events in the subducted slab may, generally, be higher than  $A_{max}$  from thrust-faulting earthquakes on the plate interface. Furthermore, a past study shows that the areas under MM intensities of IV, V, and VI in México are about four times greater for the intraplate as compared to the interplate earthquakes. These two observations explain the relatively large damage historically suffered by towns and villages in the Mexican altiplano from normal-faulting earthquakes in the subducted plate. It is quite possible that this may be the case in other subduction zones as well.

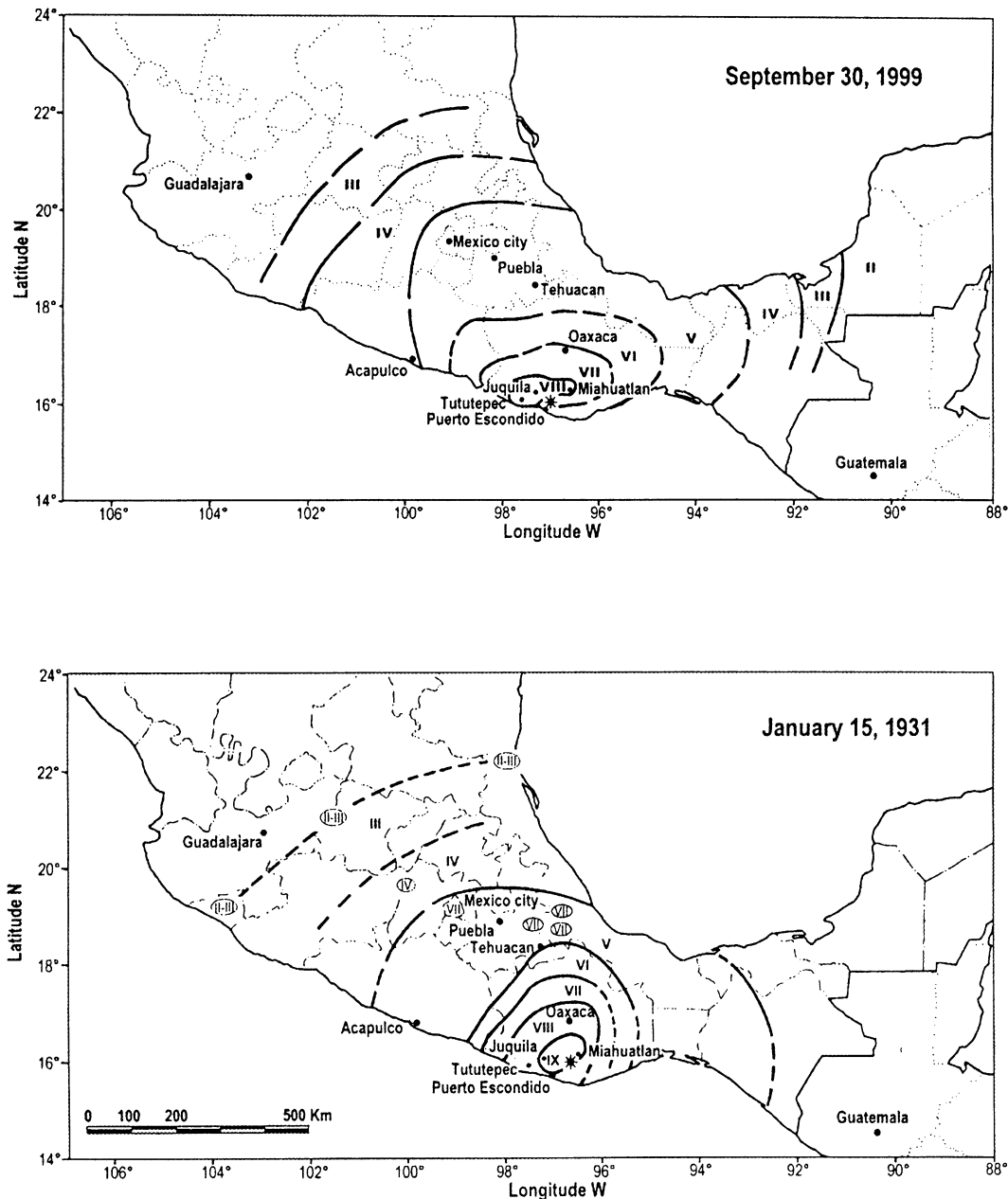
The Oaxaca earthquake, once again, underscores the need for near-real-time transmission of data from seismological and strong-motion stations in México. Had this been the case it would have permitted a quick and reliable determination of the depth and the focal mechanism of the earthquake and, hence, a better appreciation of its damage potential. As it was, it took more than two hours, until the Harvard CMT solution became available through the Internet, to know that the earthquake was an intraplate event. ■

## ACKNOWLEDGMENTS

M. Kikuchi generously provided us with his results of teleseismic body-wave inversion. We thank J. E. Ebel for a revision of the manuscript and S. Kirby for his interest in intraplate Mexican earthquakes. The dedication of the technical staffs of SSN, SISMEC, CENAPRED, and CFE to network maintenance is gratefully acknowledged. The research was partially funded by DGAPA, UNAM project IN109598, and CONACyT project 25403A.

## REFERENCES

- Astiz, L. and H. Kanamori (1988). Large intermediate-depth earthquakes and subduction process, *Phys. Earth Planet. Interiors* **53**, 80–166.
- Barrera, D.T. (1931). El temblor del 14 de enero de 1931, *Reporte Instituto de Geología*, Universidad Nacional Autónoma de México, 40 pp.
- Bouchon, M. (1982). The complete synthetics of crustal seismic phases at regional distances, *J. Geophys. Res.* **87**, 1,735–1,741.
- Brune, J.N. (1970). Tectonic stress and the spectra of seismic shear waves from earthquakes, *J. Geophys. Res.* **75**, 4,997–5,009.
- Christensen, D.H. and L.J. Ruff (1988). Seismic coupling and outer rise earthquakes, *J. Geophys. Res.* **93**, 13,421–13,444.
- Cocco, M., J.F. Pacheco, S.K. Singh, and F. Courboulex (1997). The Zihuatanejo, Mexico earthquake of December 10, 1994 ( $M =$



▲ **Figure 8.** Isoseismic maps (MM intensities) of the 1999 ( $M_w = 7.5$ ) and 1931 ( $M = 7.8$ ) normal-faulting earthquakes of Oaxaca.

- 6.6): Source characteristics and tectonic implications, *Geophys. J. Int.* **131**, 135–145.
- Gutiérrez, C. and S. Miller (1992). Isosistas del sismo del 15 de enero de 1931 (M 8) Oaxaca, México, Informe interno del Centro Nacional de Prevención de Desastres, México, D.F.
- Lay, T., L. Astiz, H. Kanamori, and D.H. Christensen (1989). Temporal variation of large intraplate earthquakes in coupled subduction zones, *Phys. Earth Planet. Int.* **54**, 258–312.
- Mikumo, T., S.K. Singh, and M. Santoyo (1999). A possible stress interaction between large thrust and normal faulting earthquakes in the Mexican subduction zone, *Bull. Seim. Soc. Am.* **89**, in press.
- Núñez-Cornu, F. and L. Ponce (1989). Zonas sísmicas de Oaxaca, México: Sismos máximos y tiempos de recurrencia para el periodo 1542–1988, *Geofs. Int. (México)* **28**, 587–641.
- Ordaz, M. and S.K. Singh (1992). Source spectra and spectral attenuation of seismic waves from Mexican earthquakes, and evidence of amplification in the hill zone of Mexico City, *Bull. Seism. Soc. Am.* **82**, 24–43.
- Ordaz, M., J.M. Jara, and S.K. Singh (1989). Riesgo sísmico y espectros de diseño en el estado de Guerrero, *Mem. VIII Congreso Nac. de Ingeniería Sísmica*, Vol. II, D40–D56, Acapulco.
- Pardo, M. and G. Suárez (1995). Shape of the subducted Rivera and Cocos Plates in southern Mexico: Seismic and tectonic implications, *J. Geophys. Res.* **100**, 12,357–12,373.
- Singh, S.K. and F. Mortera (1991). Source-time functions of large Mexican subduction earthquakes, morphology of the Benioff zone, and the extent of the Guerrero gap, *J. Geophys. Res.* **96**, 21,487–21,502.
- Singh, S.K. and M. Ordaz (1994). Seismic energy release in Mexican subduction zone earthquakes, *Bull. Seism. Soc. Am.* **84**, 1,533–1,550.

- Singh, S.K., J. Havskov, K. McNally, L. Ponce, T. Hearn, and M. Vassiliou (1980). The Oaxaca, Mexico earthquake of 29 November 1978: A preliminary report on aftershocks, *Science* **207**, 1,211–1,213.
- Singh, S.K., M. Reichle, and J. Havskov (1980). Magnitude and epicenter estimations of Mexican earthquakes from isoseismic maps, *Geofis. Int. (México)* **19**, 269–284.
- Singh, S.K., J. Havskov, and L. Astiz (1981). Seismic gaps and recurrence periods of large earthquakes along the Mexican subduction zone, *Bull. Seism. Soc. Am.* **71**, 827–843.
- Singh, S.K., M. Rodríguez, and L. Esteva (1983). Statistics of small earthquakes and frequency of occurrence of large earthquakes along the Mexican subduction zone, *Bull. Seism. Soc. Am.* **73**, 1,779–1,796.
- Singh, S.K., G. Suárez, and T. Domínguez (1985). The great Oaxaca earthquake of 15 January 1931: Lithosphere normal faulting in the subducted Cocos Plate, *Nature* **317**, 56–58.
- Singh, S.K., M. Ordaz, J.F. Pacheco, R. Quaas, L. Alcántara, S. Alcocer, C. Gutiérrez, R. Meli, and E. Ovando (1999a). A preliminary report on the Tehuacán, México earthquake of June 15, 1999 ( $M_w = 7.0$ ), *Seism. Res. Lett.* **70**, 489–504.
- Singh, S.K., M. Ordaz, J.F. Pacheco, and F. Courboux (1999b). A simple source-inversion scheme for displacement seismograms recorded at short distances, *J. Seism.*, in press.
- Valdés, C., W.D. Mooney, S.K. Singh, R.P. Meyer, C. Lomnitz, J.H. Lueterget, C.E. Helsley, B.T.R. Lewis, and M. Mena (1986). Crustal structure of Oaxaca, Mexico from seismic refraction measurements, *Bull. Seism. Soc. Am.* **76**, 547–563.
- Yagi, Y. and M. Kimkuchi (1999). Spatiotemporal distribution of source rupture process for the Mexican earthquake of September 30, 1999 (in preparation).

*Instituto de Geofísica  
UNAM*

*CU, Coyoacan 04510, México, D.F.  
México  
(S.K.S., N.S., V.K., J.F.P., T.M.)*

*Instituto de Ingeniería  
UNAM*

*CU, Coyoacan 04510, México, D.F.  
México  
(S.K.S., M.O., L.A., S.A., R.Q., E.O.)*

*Centro Nacional de Prevención de Desastres  
Delfín Madrigal 665*

*Coyoacan 04360, México, D.F.  
México  
(S.A., C.G., R.Q.)*